Belwanshi, V., Prasad, A., Toland, K., Anastasiou, K., Bramsiepe, S., Middlemiss, R., Paul, D. J. and Hammond, G. D. (2022) A Simulation Study of the Temperature Sensitivity and Impact of Fabrication Tolerances on the Performance of a Geometric Anti-Spring Based MEMS Gravimeter. In: 9th International Symposium on Inertial Sensors and Systems (INERTIAL 2022), Avignon, France, 8-11 May 2022, ISBN 9781665402828 (doi: [10.1109/INERTIAL53425.2022.9787761](https://doi.org/10.1109/INERTIAL53425.2022.9787761))

There may be differences between this version and the published version. You are advised to consult the published version if you wish to cite from it.

http://eprints.gla.ac.uk/273541/

Deposited on 24 June 2022

Enlighten – Research publications by members of the University of Glasgow
http://eprints.gla.ac.uk

A Simulation Study of the Temperature Sensitivity and Impact of Fabrication Tolerances on the Performance of a Geometric Anti-Spring Based MEMS Gravimeter

Vinod Belwanshi[1], Abhinav Prasad[1], Karl Toland[1], Kristian Anastasiou[1], Steven Bramsiepe[1], Richard Middlemiss[1], Douglas J. Paul[2] and Giles D. Hammond[1]
[1]Institute for Gravitational Research, School of Physics and Astronomy, University of Glasgow, Glasgow, UK G12 8QQ
[2]Electronics and Nanoscale Engineering, James Watt School of Engineering, University of Glasgow, Glasgow, UK, G12 8LT
email Vinod.Belwanshi@glasgow.ac.uk Abhinav.Prasad@glasgow.ac.uk Giles.Hammond@glasgow.ac.uk

***Abstract*—In this work, the effect of temperature change and fabrication tolerances observed from fabricated devices for a geometric anti-spring (GAS) based Microelectromechanical Systems (MEMS) gravimeter is modelled using Finite Element Analysis (FEA). The temperature-induced effects are analysed in terms of the temperature coefficient of deflection (TCD) for GAS flexures of varying cross-section profiles. The simulated models suggest that the maximum TCD is observed at the minimum stiffness operating points of the flexures. The models also suggest that the cross-sectional shape changes due to fabrication tolerances significantly impact the stiffness, and, hence, the resonant frequency of the devices. Interestingly, it is observed that the temperature sensitivities of the simplified models are found to be mainly dependent on the device material (Si), irrespective of the cross-sectional profiles.**

Keywords— MEMS gravimeter; temperature sensitivity; Geometrical anti-spring; FEA

I. Introduction

Microelectromechanical Systems (MEMS)-based silicon sensors have gained popularity in a variety of application areas and one of the potential applications is in gravimetry. The University of Glasgow have previously developed a relative MEMS gravimeter that uses geometrical anti-spring (GAS) based flexures to improve the acceleration sensitivity of the device [1],[2]. However, without a proper temperature control, the stability of the sensor is significantly impacted by any ambient temperature fluctuations. This is in part because silicon exhibits a negative linear temperature coefficient of Young's modulus (TCE) of around -63.83 ppm/°C [3]-[5]. A change in temperature leads to either the stiffening (when temperature decreases) or softening (when temperature increases) of the flexure springs that causes a corresponding displacement of the proof-mass. To remove the impact of temperature from the measurements, one must either monitor the temperature and regress it out during the post-processing step or implement passive or active compensation techniques. However, all these approaches have their advantages/disadvantages that need to be weighed before any implementation. In addition to temperature effects, the frequency characteristics of the devices based on the GAS flexure designs can also deviate from the pre-fabrication modelling. Fabrication of these devices use high-aspect ratio etching of features (often using the Bosch process[6]) which can potentially introduce unwanted fabrication related anomalies of the flexure's cross-sectional geometry. Considering that GAS based MEMS designs are gaining popularity in the recent years[7],[8], it is crucial to understand the impact of temperature and fabrication on working of such devices. While there has been some previous work on formulising the temperature sensitivity of GAS flexures used for test-mass suspensions in gravitational wave detectors [9],[10], a complimentary study for the MEMS scale designs and the impact of fabrication tolerances has not been adequately covered. Here, we address both the aspects using a finite-element analysis based approach.

In this paper, a simplified model of a GAS based silicon MEMS gravimeter is used. To obtain accurate estimates, the anisotropic material property of single crystal silicon is taken. The degradation in the performance of the gravimeter in terms of standard (deflection, stress) and derived (stiffness, frequency, temperature coefficient of deflection or TCD) parameters is analysed and presented. To model more realistic devices, the impact of fabrication tolerances on the change in the flexure's cross-section is also investigated. The paper is divided as follows: Section II introduces the methodology used to conduct the research work with a brief description of modelled flexure geometries, Section III describes the key results and discussions, and Section IV outlines the major findings and future directions

II. Methodology

For this study, a pair of centrally-joint 9 µm wide and 240 µm thick GAS flexures were designed with a 1.6×10^{-5} kg point mass attached where the two flexures meet (Fig. 1(a)). The geometry of the flexures, and the various boundary constraints (including the mass loading) are kept similar to the devices manufactured in the cleanroom. To assess the impact of the fabrication

anomalies, several cross-sectional wall etch-profiles (tapered (Fig. 1(c)) and “hour-glass shaped” flexures (Fig. 1(d))) were also modelled, simulated and analysed. The obtained results were compared with the ideal case where the etched walls have perfect verticality (tapered 0° (ideal)) as shown in Fig. 1(b). For the tapered wall designs of flexure, the vertical angles were taken as 0.12° (top width 9 µm and bottom width 8 µm) and 0.24° (top width 9 µm and bottom width 7 µm). To model a comprehensive scenario, an often observed hour-glass shaped flexure cross-section with 7.5 µm width in middle was also considered. The geometrical parameters for the ideal flexure are listed in Table I. These were, again, inspired from the measurements taken after fabrication of the test devices. The micro photographs of fabricated flexures of the MEMS gravimeter are presented in the Fig. 1 (e), indicating a tapered etch profile and (f), indicating an hour-glass shape respectively.

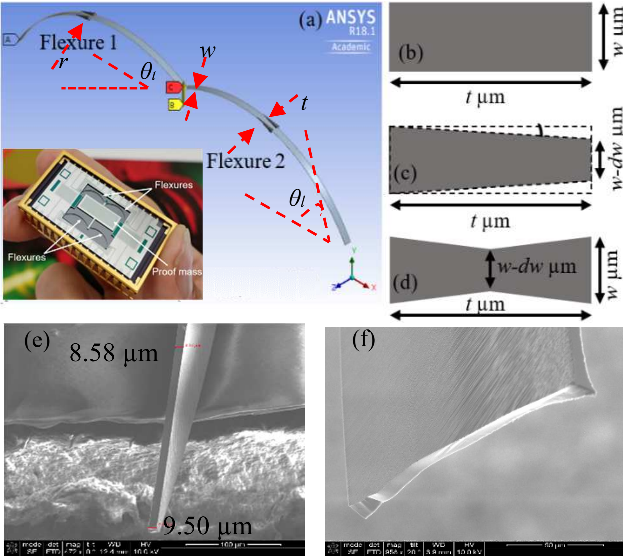

Fig. 1: (a) A simplified model and packaged MEMS gravimeter developed at Glasgow (b) the designed flexure cross-sections (c), and (d) the assumed tapered and hour-glass shaped anomaly due to the DRIE (deep reactive-ion etching) fabrication process. The microphotographs of fabricated (e) tapered (f) hour-glass shaped flexures.

TABLE I: GEOMETRICAL PARAMETERS FOR THE IDEAL GAS FLEXURE

Launch angle, θ_l (°)	**Angle at tip, θ_t (°)**	**Radius, r (µm)**	**Width, w (µm)**	**Thickness, t (µm)**
60	30	5300	9	240

For simulations, the temperature dependent material properties of anisotropic silicon were taken from the literature [3]–[5]. The anisotropic material properties of silicon are defined by a 6 × 6 stiffness matrix which comprises of three distinct stiffness components- c_{11}, c_{12}, and c_{44}. Using TCE values for the respective components, the temperature-dependent stiffness matrix can be generated. The stiffness matrix elements and the corresponding TCE values are listed in Table II.

TABLE II: THE ANISOTROPIC MATERIAL PROPERTIES OF SILICON USED IN THE SIMULATION MODELS

Materials	**Young’s modulus at 25 °C (GPa)**		**TCE (ppm/°C)**
Anisotropic Silicon	c_{11}	165.64	-73.3
	c_{12}	63.94	-91.6
	c_{44}	79.51	-60.1

Anisotropic silicon was used to simulate the performance (deflections and induced stresses) of the simplified model of gravimeter using the FEA simulation. The stiffness, frequency and TCD were derived using the simulated deflection as below.

The equivalent stiffness of the flexure was calculated using Eq. 1 for all the flexure designs.

$$k = \frac{\Delta F}{\Delta y} = \frac{m\Delta g}{\Delta y} \qquad (1)$$

The frequency was calculated using Eq. 2 (Fig. 4 (b)).

$$f = \frac{1}{2\pi}\sqrt{\frac{k}{m}} \qquad (2)$$

where, k, f, Δy, m, ΔF, and Δg are stiffness, frequency, change in deflection, mass, change in force and change in acceleration, respectively.

Change in the deflection under the influence of the temperature was simulated and analysed in terms of the TCD for all the flexure shapes. The TCD was calculated as in Eq. 3.

$$TCD = \frac{(d_{T_1} - d_{T_0})}{d_{T_0}} \frac{1}{T_1 - T_0} \qquad (3)$$

Temperature sensitivity in terms of the µGal/mK was calculated as given in Eq. 4.

$$\frac{\Delta g}{\Delta T} = \frac{(d_{T_1} - d_{T_0})}{T_1 - T_0} w^2 \qquad (4)$$

Where, d_{T_1} and d_{T_0} are deflections at T_1 and T_0 temperatures respectively, $w = 2\pi f$, $\frac{\Delta g}{\Delta T}$ is temperature sensitivity in terms of the Gal/K.

For every loading condition, and for each flexure design, the temperature of the silicon was varied in the range of -50 °C to 50 °C. The resulting deflections for each temperature step were recorded and a TCD value with respect to the deflection at room temperature was calculated and presented in the result sections.

III. RESULTS AND DISCUSSIONS

The simulations were performed for various flexure wall profiles. The deflection and the stress profiles of the silicon GAS flexures with a width of 9 µm and under the applied acceleration of 9.81 m/s^2 (~1 g) are shown in Fig. 2. A maximum deflection (~1226 µm) and a maximum induced stress (165 MPa) were observed at the centre where the tips of the two flexures are joined, as can be seen in Fig. 2 (a) and (b), respectively.

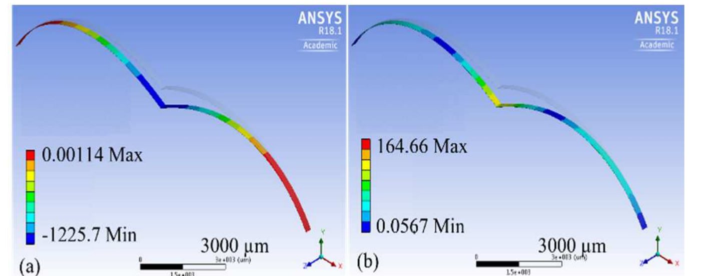

Fig. 2: (a) The deflection and (b) the induced stress profiles of the silicon GAS flexure after a load of 9.81 m/s^2 is applied in direction of interest.

A. Deflection and induced stress profile under applied acceleration

Deflection under the varying load conditions were analysed for the wall profiles as mentioned above. As expected, the deflection of flexures exhibited a nonlinear non-Hookian behaviour as the applied acceleration increases (this is the inherent property of GAS flexures which become softer when the loading increases). Interestingly, and as expected the deflection was found to be increasing with an increase in the tapered angle of flexures (Fig. 3 (a)). The maximum deflection of flexures increased by almost a factor of 2 from 1226 µm to 2341 µm when the taper increased to 0.24° under 1g acceleration. The hour-glass shaped flexure also showed an increased deflection when compared to the ideal flexure. The induced stress consistently demonstrated a nonlinear behaviour with applied acceleration. An increase in the induced stresses were observed with an increase in the tapered angle. (Fig. 3(b)). The change in the deflection and induced stress could be attributed to the decrease in the effective thickness of flexures (more missing material due to the non-ideal etching process). It was also observed that the maximum induced stresses are in the range of 164-214 MPa, which is well below the fracture stress of Si (~6.1 GPa) [11].

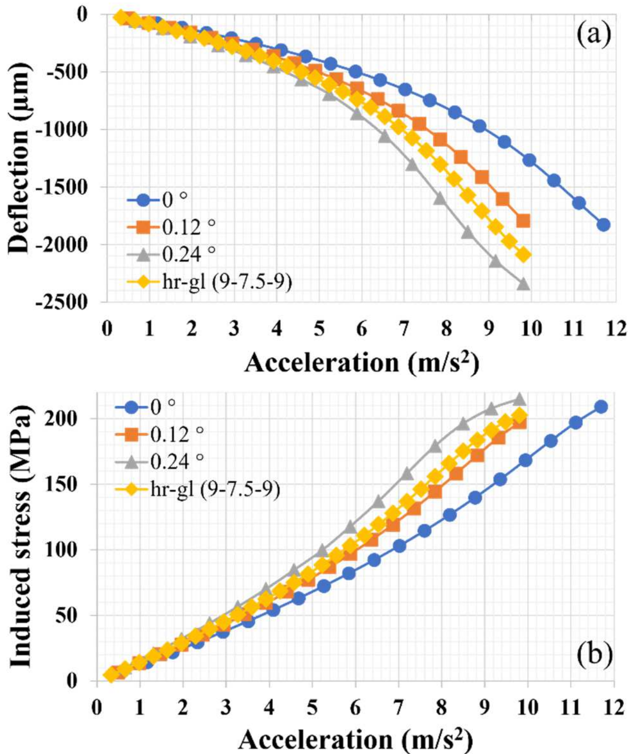

Fig. 3: (a) Deflection vs acceleration (b) Induced stress vs acceleration for varying shape of flexure cross-sections at 25 °C. The blue-circle, orange-square, grey-triangle and yellow-diamond curves are ideal (0.0° tapered), 0.12° 0.24° and hour-glass shaped tapered flexures (applicable elsewhere).

The minimum stiffness for the ideal flexure was calculated using Eq. 1 as 0.048 N/m occurring at a loading of 11.115 m/s^2 resulting in a resonant frequency of 8.76 Hz (using Eq. 2). Similarly, stiffness, frequency, and acceleration at operating points (minimum stiffness point) are calculated for all the other cross-sectional shape of flexures and listed in Table III. The flexures stiffness and frequency under applied acceleration are presented in Fig. 4. As can be seen from Fig. 4, stiffness and frequency are decreasing as the applied acceleration increases until the minimum stiffness or frequency of the flexures is reached. The minimum stiffness point (or, the operating point) is identified as the point where the GAS gravimeters should ideally operate as the stiffness becomes relatively insensitive to loading changes and a simple Hooke's spring model could be used for calculating inertial accelerations for modest displacements. It is observed that the stiffness and the frequency of the flexure also change significantly with a change in the flexure's cross-sections.

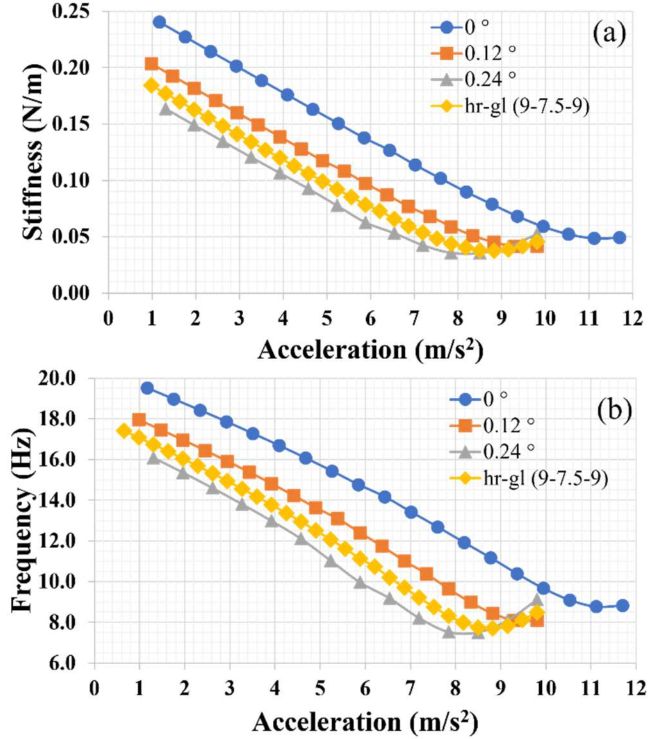

Fig. 4: (a) Stiffness vs acceleration (b)frequency vs acceleration for varying flexure's cross-section at 25 °C.

TABLE III: VALUES OF STIFFNESS, FREQUENCY AND APPLIED ACCELERATION AT THE OPERATING POINT (AT 25 °C)

Geometry	Stiffness (N/m)	Frequency (Hz)	Acceleration (m/s^2)
0 °	0.048	8.76	11.115
0.12 °	0.041	8.08	9.81
0.24 °	0.036	7.51	8.50
hr-gl(9-7.5-9)	0.038	7.70	8.83

The TCD was calculated using Eq. 3. It was observed that the TCD increases with applied acceleration until the minimum stiffness or frequency is achieved and beyond this point, it starts decreasing. The maximum TCD was observed at the operating point for all flexures and remains nearly identical for all flexure's shape at the minimum stiffness (Fig. 5).

B. Temperature sensitivity

Temperature sensitivity was calculated using Eq. 4. It can –

-be seen from Fig. 6 that temperature sensitivity in terms of the μGal/mK (1 μGal = 1 ng) increases with an increase in the load. Also, a nearly identical temperature sensitivity for all the flexures was observed. Hence, it can be concluded that the temperature sensitivity is mainly dependent on the material used for the flexure irrespective of the cross section of flexures. However, the operating point is significantly affected by the flexure's cross section. These results clearly indicate that there is a trade-off in setting the minimum stiffness point. On one hand, at minimum stiffness point, a Hookian behaviour (for small loads) and a high sensitivity is observed, it also has the worst temperature sensitivity.

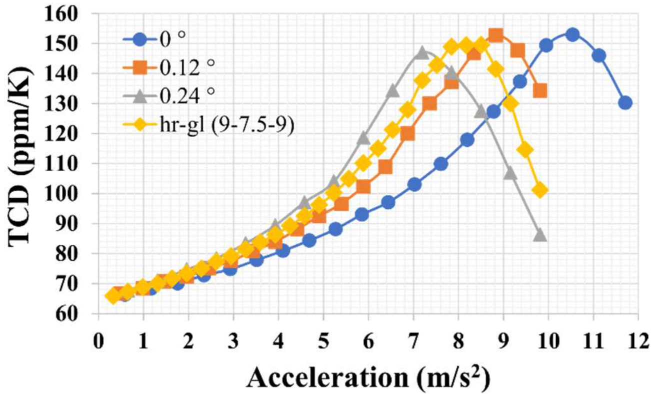

Fig. 5: TCD of silicon GAS based MEMS gravimeter.

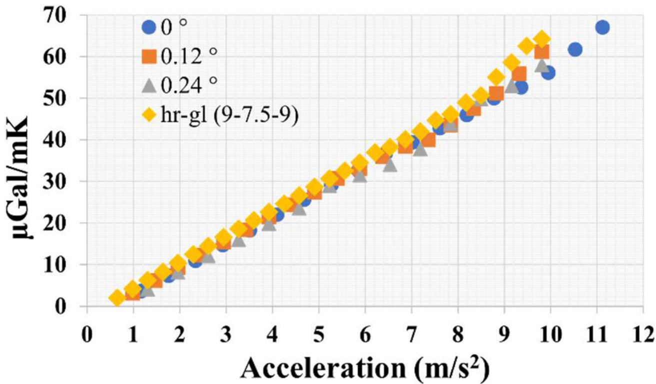

Fig. 6: The temperature sensitivity of the modelled flexures in terms of the μGal/mK units.

IV. Conclusions

In this work, a simulation study of a simplified model of a MEMS gravimeter is presented. Both, the temperature effects and the impact of fabrication tolerances on the device parameters like deflection, stress, stiffness, frequency, and acceleration sensitivity are tabulated. Fabrication anomalies were found to significantly impact the location of the operating point. The temperature coefficient of deflection for all the flexure shapes showed a maximum value at the minimum stiffness (the operating point) of flexures. This indicates that GAS based devices need proper temperature control, either through active or through passive techniques, to overcome such high temperature sensitivities. Temperature sensitivity was found nearly identical for all the flexures which suggests it is dependent mostly on the material of the flexure. The inherent temperature sensitivity of the flexures is the biggest challenge in using these devices for the precise measurement of gravity and the seismic activity of the earth. We hope that this initial simulation study will provide a useful starting point when it comes to the selection of suitable substrate materials and the choice of compensation techniques for improving the temperature sensitivity of GAS based devices.

Acknowledgment

The authors would like to thank the following funders towards this project: Royal Society Paul Instrument Fund, STFC grant number ST/M000427/1, UK National Quantum Technology Hub (EP/M01326X/1, EP/T001046/1), EU H2020 project 'NEWTON-g' (H2020-FETOPEN-1-2016-2017) and the Royal Academy of Engineering grants CiET2021_123 and RF/201819/18/83.

References

[1] R. P. Middlemiss, A. Samarelli, D. J. Paul, J. Hough, S. Rowan, and G. D. Hammond, "Measurement of the Earth tides with a MEMS gravimeter," Nature, vol. 531, no. 7596, pp. 614–617, 2016, doi: 10.1038/nature17397.

[2] A. Prasad et al., "A Portable MEMS Gravimeter for the Detection of the Earth Tides," in 2018 IEEE SENSORS, 2018, pp. 1–3. doi: 10.1109/ICSENS.2018.8589884.

[3] R. Melamud et al., "Temperature-insensitive composite micromechanical resonators," Journal of Microelectromechanical Systems, vol. 18, no. 6, pp. 1409–1419, 2009, doi: 10.1109/JMEMS.2009.2030074.

[4] M. A. Hopcroft, W. D. Nix, and T. W. Kenny, "What is the Young's modulus of silicon?," Journal of Microelectromechanical Systems, vol. 19, no. 2, pp. 229–238, 2010, doi: 10.1109/JMEMS.2009.2039697.

[5] C. Bourgeois, J. Hermann, N. Blanc, N. F. de Rooij, and F. Rudolf, "Determination of the elastic temperature coefficients of monocrystalline silicon," International Conference on Solid-State Sensors and Actuators, and Eurosensors IX, Proceedings, vol. 2, pp. 92–95, 1995, doi: 10.1109/sensor.1995.721752.

[6] F. Laermer and A. Schilp, "Method of anisotropically etching silicon," US Patent No 5501893, Mar. 26, 1996

[7] B. A. Boom et al., "Nano-G accelerometer using geometric anti-springs," in 2017 IEEE 30th International Conference on Micro Electro Mechanical Systems (MEMS), 2017, pp. 33–36. doi: 10.1109/MEMSYS.2017.7863332.

[8] H. Zhang, X. Wei, Y. Gao, and E. Cretu, "Frequency characteristics and thermal compensation of MEMS devices based on geometric anti-spring," Journal of Micromechanics and Microengineering, 2020, doi: 10.1088/1361-6439/ab9203.

[9] A. T. G. Cella, V. Sannibale, R. DeSalvo, S.Ma´ rka, "Monolithic geometric anti-spring blades," Nuclear Instruments and Methods in Physics Research, vol. 540, pp. 502–519, 2005, doi: 10.1016/j.nima.2004.10.042.

[10] M. Blom, "Seismic attenuation for advanced virgo Vibration isolation for the external injection bench," Ph. D. Thesis, Vrije Universiteit Amsterdam, Amsterdam, The Netherlands, 2015.

[11] F. Ericson and J. Å. Schweitz, "Micromechanical fracture strength of silicon," Journal of Applied Physics, vol. 68, no. 11, pp. 5840–5844, 1990, doi: 10.1063/1.346957.